

A Possible Four-Month Periodicity in the Activity of FRB 20240209A

ARPAN PAL ¹

¹*National Centre for Radio Astrophysics, Tata Institute of Fundamental Research, S. P. Pune University Campus, Ganeshkhind, Pune, 411007*

ABSTRACT

Fast Radio Bursts (FRBs) are millisecond-duration radio transients from distant galaxies. While most FRBs are singular events, repeaters emit multiple bursts, with only two—FRB 121102 and FRB 180916B—showing periodic activity (160 and 16 days, respectively). FRB 20240209A, discovered by CHIME-FRB, is localized to the outskirts of a quiescent elliptical galaxy ($z = 0.1384$). We discovered a periodicity of ~ 126 days in the activity of the FRB 20240209A, potentially adding to the list of extremely rare periodic repeating FRBs. We used auto-correlation and Lomb-Scargle periodogram analyses, validated with randomized control samples, to confirm the periodicity. The FRB’s location in an old stellar population disfavors young progenitor models, instead pointing to scenarios involving globular clusters, late-stage magnetars, or low-mass X-ray binaries (LMXBs). Though deep X-ray or polarimetric observations are not available, the localization of the FRB and a possible periodicity points to progenitors likely to be a binary involving a compact object and a stellar companion or a precessing/rotating old neutron star.

Keywords: Fast Radio Bursts, Periodic FRBs, Low-mass X-ray Binaries

1. INTRODUCTION

Fast Radio Bursts (FRBs; Lorimer et al. 2007) are mysterious astronomical events that are defined by radio flashes that last milliseconds and come from extragalactic origins (Tendulkar et al. 2021; Ravi et al. 2022). Repeating FRBs (Spitler et al. 2016), which release several bursts over time, and non-repeating FRBs, which have been seen as solitary, single events, are the two different classifications into which these bursts come. The physical processes that underlie FRB emission are still unknown. There are currently ~ 60 repeating and ~ 800 ¹ non-repeating FRBs known to exist. FRB 121102 (Spitler et al. 2014) and FRB 180916B (CHIME/FRB Collaboration et al. 2019) are the only two sources in the repeating population that show periodic behavior. While FRB 180916B exhibits a shorter periodic pattern with bursts occurring every 16 days (Chime/Frb Collaboration et al. 2020), FRB 121102 exhibits an activity cycle of 160 days (Rajwade et al. 2020). Although the majority of repeating FRBs do not display clear periodicity, the existence of these two periodic sources challenges theoretical models that propose completely stochastic burst generation mechanisms. Using isolated compact

object mechanisms to generate periodicity on timescales of weeks to months is very difficult (Chime/Frb Collaboration et al. 2020). Two primary alternative theories have surfaced to satisfy this theoretical constraint: precession of highly magnetic neutron stars undergoing periodic flaring episodes (Levin et al. 2020a; Zanazzi & Lai 2020) and binary orbital motion (Lyutikov et al. 2020; Ioka & Zhang 2020). Month-scale periodicity detection and constraint necessitate long-term, intensive observational follow-up.

With its four cylindrical reflector arrays offering a wide field of view of 200 square degrees (CHIME/FRB Collaboration et al. 2018), the Canadian Hydrogen Intensity Mapping Experiment (CHIME; CHIME/FRB Collaboration et al. 2018) is in a unique position to accomplish this objective. Its ability to continuously watch the sky guarantees thorough detection of burst activity beyond a fluence threshold of 1 Jyms (CHIME/FRB Collaboration et al. 2018), which makes it the perfect tool for both finding new FRBs and carrying out objective, long-term monitoring of established sources.

FRB 20240209A was initially detected by the CHIME-FRB collaboration (Shah & CHIME/FRB Collaboration 2024). Subsequent baseband observations with CHIME and the outtrigger KKO station (Lanman et al.

¹ <https://www.wis-tns.org/>

2024) revealed that FRB 20240209A is localized to the peripheral regions of a quiescent galaxy at redshift $z = 0.1384$ (Shah et al. 2025). The offset of the burst from the host galactic center is significant, measuring 40 ± 5 kpc (68% confidence), and the host-normalized offset is $5.13 \pm 0.6R_{\text{eff}}$ (Shah et al. 2025). FRB 20240209A differs from the typical FRB population, which originates primarily from star-forming galaxies with offsets of ≤ 10 kpc (Heintz et al. 2020; Mannings et al. 2021; Bhandari et al. 2022; Gordon et al. 2023; Sharma et al. 2024), due to its remarkable galactic offset and its association with a luminous, quiescent host galaxy. Notably, this FRB has the second-highest host-normalized offset and the largest absolute host-galaxy offset, only surpassed by FRB 20200120E, which was located to a globular cluster in M81 (Bhardwaj et al. 2021; Kirsten et al. 2022). Furthermore, it represents the first clear association of an FRB with an elliptical galaxy (Shah et al. 2025). The burst characteristics include a dispersion measure of $176.57(3)$ pc cm $^{-3}$ and a rotation measure (RM) of $< 10 \text{ radm}^{-2}$ for the two reported CHIME bursts (Shah & CHIME/FRB Collaboration 2024).

In this paper, we make use of the publicly available CHIME-FRB repeater database, and report the discovery of a possible periodicity in the activity of the FRB 20240209A. We organize the paper as follows, we report the burst database and periodicity search in section 2 describing the core results and methods. We conclude discussing the implications over the possible progenitor models in section 3.

2. BURST DATASET AND PERIODICITY SEARCH

The repeating FRB is continuously monitored by CHIME, with burst detections, arrival times, and DM measurements regularly updated in the CHIME-FRB repeaters’ public database (<https://www.chime-frb.ca/repeaters>). Using the database, we conducted a systematic search for periodicity in the burst activity of FRB 20240209A.

On March 14, 2025, we downloaded the CHIME-FRB VOE services’ repeaters’ data, this serves as the foundation of our analysis. To look for periodicity, we implemented the autocorrelation function (ACF) analysis in the time series. The normalized ACF was computed by correlating the signal with itself at increasing time lags, with peaks in the resulting function corresponding to potential periodic components. The burst’s ACF analysis showed a notable peak at 128.5 ± 6 days, suggesting that the burst activity may be recurrent. The normalized ACF indicated a relatively strong periodic signal, with this peak showing a prominence of 0.4 (Fig. 1).

To confirm, we also performed a Lomb-Scargle (Scargle 1982) periodogram analysis for the available bursts of the FRB 20240209A. The Lomb-Scargle periodogram performs a least-squares fit of sinusoids to the data, evaluating the power at each test frequency. Unlike simpler methods, it’s specially designed to handle gaps or irregular timing in the measurements (Scargle 1982). The periodogram was computed over a frequency range corresponding to periods between 1 and 300 days. We produced random time-stamps between the days of the first and last detection of the FRB and from the times when the FRB was situated inside the CHIME field of view. We first selected random days inside the first and last detection of the FRB. We then calculated the transit time and periods on those specific dates using the CHIME-FRB transit calculator². The list was supplied to the bootstrapping script which does random pickups from the times when the FRB was up in the CHIME sky. Also, when the script picks dates which are not exactly in the dictionary, the transit time was corrected approximately using the sidereal correction factor of 3 minutes and 56 seconds. Now with random 10,000 trials of the time stamps, bootstrap analysis was used to determine statistical significance, with confidence levels set at 1σ (68.27%), 2σ (95.45%), and 3σ (99.73%). At 119 ± 13 days, the analysis showed a dominant peak that was higher than the 3σ confidence level (power ≥ 0.79).

With the ACF and Lomb-Scargle values agreeing within their uncertainties, the period obtained using both approaches demonstrates excellent consistency. Clusters of strong activity interspersed with comparatively quiet periods are how this period shows up in the burst arrival times. Our dataset shows three primary active phases, with MJD 60360, 60478, and 60630 in their centers.

Further validation of the periodic behaviour was performed through epoch folding analysis (Similar method introduced in Stellingwerf 1978 and following the methods described in Leahy et al. 1983), which yielded a peak at $P = 128.8 \pm 14$ days. Epoch folding in FRB periodicity analysis involves dividing potential periods into phase bins and measuring how bursts cluster when “folded” at different trial periods. When the correct period is found, bursts cluster in specific phase bins rather than being uniformly distributed. The Pearson chi-square test quantifies this non-uniformity by comparing observed burst counts (N_i) in each phase bin against expected counts (E_i) under uniform distribution (Eq. 1) A higher chi-square value indicates a periodic

² <https://www.chime-frb.ca/astronomytools>

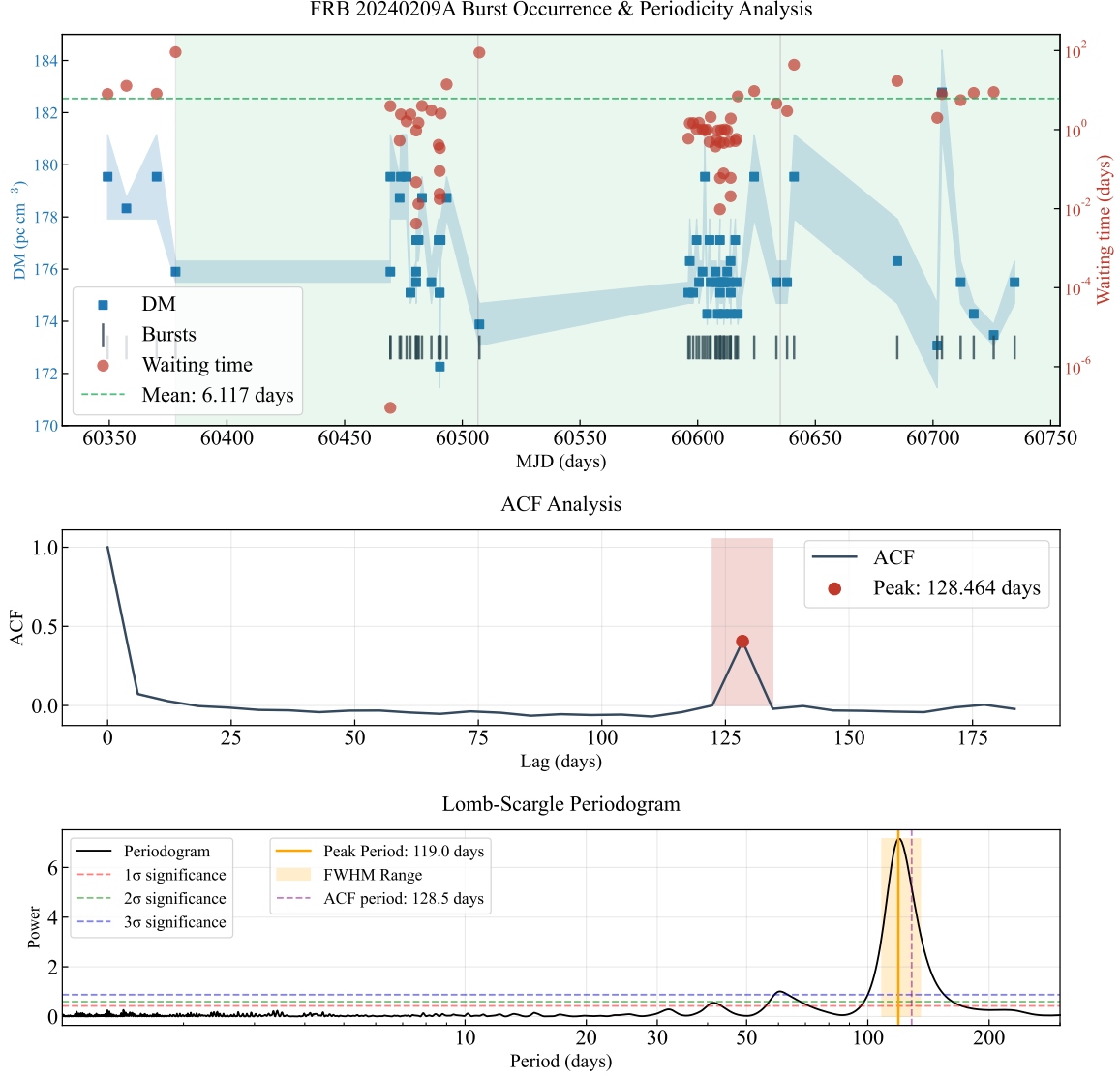


Figure 1. Temporal and periodicity analysis of FRB 20240209A. Top panel: Burst occurrence timeline showing the DM variations (blue squares), individual bursts (black ticks), and waiting times between consecutive bursts (red circles) as a function of Modified Julian Date (MJD). The mean waiting time of 5.886 days is indicated by the green dashed line. The filled blue regions show the error bars on the detected DM. The shaded green region shows the measured period visually and each box has a width of the measured ACF periodicity. Middle panel: Auto-correlation function (ACF) analysis revealing a significant peak at 123.615 days (red point with pink shaded uncertainty region). Bottom panel: Lomb-Scargle periodogram showing a strong peak at 126.6 days, with 1σ , 2σ , and 3σ significance levels indicated by horizontal dashed lines. The FWHM range of the peak (yellow shaded region) and the ACF-derived period (purple dashed line) demonstrate the consistency between different periodicity analysis methods.

signal, with the highest value typically corresponding to the true period.

$$\chi^2 = \sum_{i=1}^n \frac{(N_i - E_i)^2}{E_i} \quad (1)$$

The uncertainty is derived from the full width at half maximum (FWHM) of the χ^2 peak (shaded region in Fig. 2). The epoch folding method splits the time series into phase bins using trial periods, computing a χ^2

statistic to measure deviations from uniform distribution. The peak period agrees with both Lomb-Scargle (119 ± 13 days) and ACF (128.5 ± 6 days) results within the uncertainties. We also have folded the profile using the periodicity of 128.8 days and the folded profiles shows primary concentrations starting at phases $\phi \sim 0.0$ and $\phi \sim 0.9$ and a noticeable activity gap between $\phi \sim 0.3 - 0.6$ and from $\sim 0.65 - 0.9$. The folded

profile shows the highest number of bursts in the beginning and the end of the activity phase.

From the Tab. 2, the bursts have different detection significances which is unlikely to significantly impact the periodicity measurements. We do not have any estimates on the burst fluence from the CHIME VOE database but most of the bursts were reported on Shah et al. (2025) where the bursts fluence ranges from 7.4 - 324.9 Jy.ms. The CHIME FRB has a fluence complete limit of 1 Jy.ms CHIME/FRB Collaboration et al. (2018). Though, the possibility of missing a broad fainter population can not be ruled out, the burst activity would still be periodic in terms of energy scales.

3. IMPLICATIONS ON THE PROGENITOR MODELS

FRB 20240209A has been proposed to be possibly associated with a globular cluster in its host galaxy (Shah et al. 2025). The observed host dispersion measure and comparison of offsets with soft-gamma-ray repeaters make alternative scenarios, such as an undetected dwarf galaxy or a kicked-off progenitor, less plausible (Shah et al. 2025). Progenitor models incorporating elderly star populations, such as magnetars generated by accretion-induced collapse of white dwarfs (WDs), merger-induced collapse of WD-WD binaries, NS-WD systems, or NS-NS binaries, are especially favored in the globular cluster environment (Shah et al. 2025).

Given their demonstrated prevalence in globular clusters, low-mass X-ray binaries (LMXBs) and ultraluminous X-ray sources (ULXs) (Clark 1975; Maccarone et al. 2007; Dage et al. 2021; Sridhar et al. 2021) are other promising candidates. The periodic character of the burst activity can suggest of a binary system. The 126 days periodicity disfavors binaries with both compact objects due to expected shorter time scales (Postnov & Yungelson 2014). It may hint towards a binary system involving a compact object and a star partner. Either the compact object itself or the interaction of magnetic fields with material stripped from the companion star could be the source of FRB emission in such situations. (Sridhar et al. 2021; Lyutikov et al. 2020; Ioka & Zhang 2020)

Other possibilities also remain open as the periodicity can be attributed to the precession (Levin et al. 2020a; Zanazzi & Lai 2020) or rotational motion of old stage magnetars (Beniamini et al. 2020; Xu et al. 2021; Beniamini et al. 2023). The nature of this source will need to be further constrained by future in-depth polarimetric investigations, particularly including measurements of position angle variations. For both the binary and pre-

cessing models, a shorter time-scale periodicity is also expected due to the spin of the magnetar itself (Beniamini et al. 2023) but currently the limited daily exposure with CHIME can not constrain a periodicity of more than 15-25 minutes (assuming daily exposure of 74 minutes). Facilities with no bound on the exposure time can be well suited to look for these short scale periods in the next expected burst activity window. If the FRBs are getting generated through interactions of the ablated material and the motion of the magnetar, a flat or slowly varying polarization angle (PA) swing can be expected if the magnetic field configuration does not change with time. However, in the case of precession and rotation, the PA will have an imprint on them. For the precession, if the smaller scale periodicity is found, the PA is expected to exhibit a swing in the magnetar's repeating timescale. Same holds for the rotation but in this we can expect a much slower and gradual swing, 128 days being attributed to the periods of the magnetar.

Later epochs (Fig. 1) reveal increased burst activity for FRB 20240209A, with the most recent events in January and February 2025 showing a decline in activity. This pattern may indicate that FRB formation is driven by interactions between ablated material and a compact object in a binary system. This variation in burst rate could be explained by changes in the companion wind density or velocity, which affects the number of particles entering the magnetosphere of the neutron star through the funnel interface (Wada et al. 2021). According to the binary comb model (Ioka & Zhang 2020; Wada et al. 2021), these variations could create aurora-like particle flows that alter emission characteristics without requiring rapid orbital evolution. By continuing to observe the source's periodic behavior over an extended period of time, we may detect changes in dispersion measure that would provide a stronger signature of the binary interaction.

The FRB's low reported rotation measure (RM) indicates that it originated in or propagated through a turbulent medium. Comprehensive RM information about this source is currently missing from the CHIME-repeaters database. Important information about the local environment and the underlying progenitor mechanism may be revealed by a thorough analysis of RM variations across detected bursts (Wang et al. 2022).

The dispersion measure (DM), available through the database, exhibits periodic modulation within the activity windows. While the magnetar-Be star binary model (Wang et al. 2022), which successfully explains the RM variations in FRB 20201124A with its characteristic zig-zag pattern, predicts a monotonic increase followed by a decrease in DM (Fig. 3 in Wang et al.

FRB 20240209A Periodicity Analysis (P = 128.8 days)

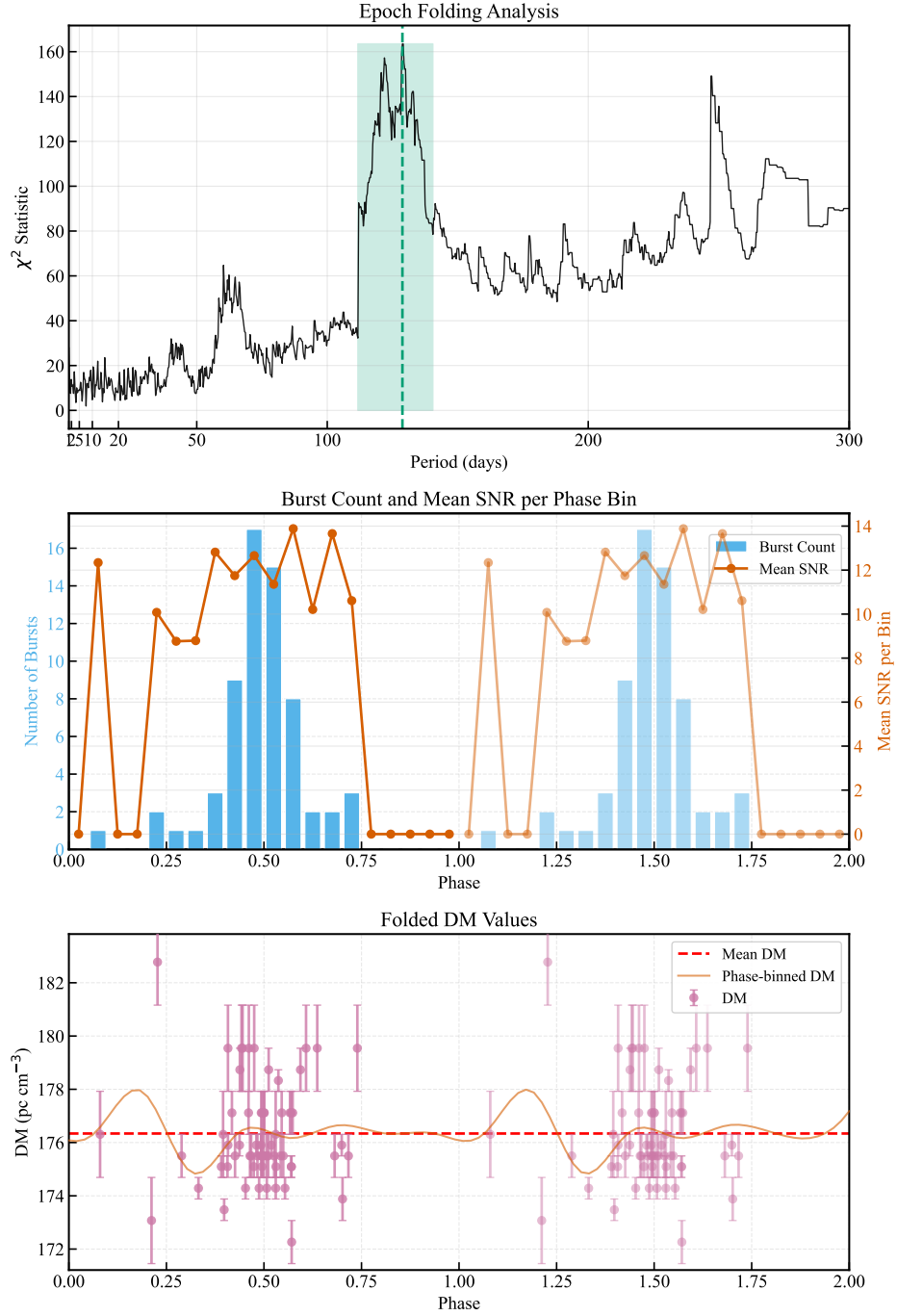


Figure 2. Periodicity analysis of FRB 20240209A using the epoch folding method. Top panel: The χ^2 statistic as a function of trial periods, showing a significant peak at 128.8 ± 15.4 days (marked by the green dashed line with green shaded region indicating the uncertainty). Middle panel: The total burst count distribution folded at the best-fit period of 128.8 days is shown in blue. The mean SNR across every phase interval is shown in a red line connecting the red dots. Bottom panel: Evolution of the DM after folding with the period of 128.8 days is shown in violet circles, with the phase averaged DM is shown as orange line. The average DM is shown in dashed red line.

2022). The FRB 20240209A displays distinct oscillatory behavior. Notably, as seen in Fig 1 (top panel), the DM exhibits a similar modulation pattern throughout

all activity phases. A decreased DM value starts the pattern, which then follows an increase, then a reduction, and then several periodic modulations (especially

in the second and third activity phases), and eventually a decline. The electron density structure of the ablated material in the disk of the binary system may be traced by this behavior. The period folded DM also shows distinct oscillatory behaviour (Fig. 2 Bottom Panel). Since interactions between the compact object and its partner are likely to cause persistent X-ray emission in such systems, deep X-ray follow-up observations will be essential for constraining the binary progenitor concept (Kirsten et al. 2022). But the even for the current state of the art telescopes like Chandra, 1 Ms is needed to reach 10^{39} ergs s^{-1} , while that can constrain the progenitor if it is a Ultraluminous X-ray Binary (Sivakoff et al. 2005; Pearlman et al. 2025) but way above if the progenitor is an late-stage magnetars ($10^{29} - 10^{36}$ ergs s^{-1} ; Coti Zelati et al. 2018), extragalactic millisecond pulsars ($10^{34} - 10^{37}$ ergs s^{-1} ; Klingler et al. 2018; Gotthelf et al. 2021), and LMXBs ($10^{30} - 10^{39}$ ergs s^{-1} ; Pearlman et al. 2025).

The FRB position was monitored by the CHIME/FRB for quite a long time before the discovery of the FRB in 2024. The sudden activation can be possibly attributed to magnetic field reconfiguration in an old magnetar or the onset of interactions in a binary system that reached a critical threshold. In the binary scenario, material ablation from the companion star may have only recently begun feeding the magnetosphere of the compact object, triggering the FRB mechanism. Alternatively, in a precessing magnetar model, the emission beam may have only recently aligned with our line of sight after years of pointing elsewhere.

The localized position of FRB 20240209A was continuously monitored by CHIME/FRB for several years before its sudden discovery in 2024. This abrupt activation can be potentially explained through multiple progenitor models. In the binary scenario, the system may have reached a critical orbital configuration where material ablation from the companion star began feeding the magnetosphere of the compact object, triggering

the FRB mechanism (Ioka & Zhang 2020; Zhang 2020). If the source is a rotating or precessing old-stage magnetar, the emission beam may have only recently aligned with our line of sight. Or, the sudden "switch-on" could represent a magnetic field reconfiguration event in the magnetar (Szary et al. 2015; Beniamini & Kumar 2020), where rapid crustal failures or magnetospheric instabilities trigger coherent radio emission that was previously absent. These magnetic reconfigurations can occur stochastically or be triggered by external perturbations. A single large-scale rearrangement of the internal magnetic field can initiate a large-angle free precession (Levin et al. 2020b).

The discovered possible ~ 4 -month periodicity and the FRB's substantial offset from its host galaxy provide compelling evidence for a binary origin of the progenitor, most likely comprising a compact object-stellar companion system. Though the currently available data can not differentiate surely between the other possibilities being a old stage rotating/precessing magnetar. The data only comprises of 2 full periods, which is just sufficient to probe any periodicity. Hence, comprehensive radio monitoring campaigns remain essential to definitively confirm the periodicity, especially with polarization to weigh all the progenitor models and constrain.

4. ACKNOWLEDGEMENTS

We acknowledge use of the CHIME/FRB Public Database, provided at <https://www.chime-frb.ca/> by the CHIME/FRB Collaboration. This research has made use of NASA's Astrophysics Data System Bibliographic Services. This research has made use of the NASA/IPAC Extragalactic Database (NED), which is operated by the Jet Propulsion Laboratory, California Institute of Technology, under contract with the National Aeronautics and Space Administration.

5. DATA AVAILABILITY

The data is publicly available on CHIME repeaters' database.

REFERENCES

- Beniamini, P., & Kumar, P. 2020, MNRAS, 498, 651, doi: [10.1093/mnras/staa2489](https://doi.org/10.1093/mnras/staa2489)
- Beniamini, P., Wadiasingh, Z., Hare, J., et al. 2023, MNRAS, 520, 1872, doi: [10.1093/mnras/stad208](https://doi.org/10.1093/mnras/stad208)
- Beniamini, P., Wadiasingh, Z., & Metzger, B. D. 2020, MNRAS, 496, 3390, doi: [10.1093/mnras/staa1783](https://doi.org/10.1093/mnras/staa1783)
- Bhandari, S., Heintz, K. E., Aggarwal, K., et al. 2022, AJ, 163, 69, doi: [10.3847/1538-3881/ac3aec](https://doi.org/10.3847/1538-3881/ac3aec)
- Bhardwaj, M., Gaensler, B. M., Kaspi, V. M., et al. 2021, ApJL, 910, L18, doi: [10.3847/2041-8213/abeaa6](https://doi.org/10.3847/2041-8213/abeaa6)
- CHIME/FRB Collaboration, Amiri, M., Bandura, K., et al. 2018, ApJ, 863, 48, doi: [10.3847/1538-4357/aad188](https://doi.org/10.3847/1538-4357/aad188)
- CHIME/FRB Collaboration, Andersen, B. C., Bandura, K., et al. 2019, ApJL, 885, L24, doi: [10.3847/2041-8213/ab4a80](https://doi.org/10.3847/2041-8213/ab4a80)

- Chime/Frb Collaboration, Amiri, M., Andersen, B. C., et al. 2020, *Nature*, 582, 351, doi: [10.1038/s41586-020-2398-2](https://doi.org/10.1038/s41586-020-2398-2)
- Clark, G. W. 1975, *ApJL*, 199, L143, doi: [10.1086/181869](https://doi.org/10.1086/181869)
- Coti Zelati, F., Rea, N., Pons, J. A., Campana, S., & Esposito, P. 2018, *MNRAS*, 474, 961, doi: [10.1093/mnras/stx2679](https://doi.org/10.1093/mnras/stx2679)
- Dage, K. C., Kundu, A., Thygesen, E., et al. 2021, *MNRAS*, 504, 1545, doi: [10.1093/mnras/stab943](https://doi.org/10.1093/mnras/stab943)
- Gordon, A. C., Fong, W.-f., Kilpatrick, C. D., et al. 2023, *ApJ*, 954, 80, doi: [10.3847/1538-4357/ace5aa](https://doi.org/10.3847/1538-4357/ace5aa)
- Gotthelf, E. V., Safi-Harb, S., Straal, S. M., & Gelfand, J. D. 2021, *ApJ*, 908, 212, doi: [10.3847/1538-4357/abd32b](https://doi.org/10.3847/1538-4357/abd32b)
- Heintz, K. E., Prochaska, J. X., Simha, S., et al. 2020, *ApJ*, 903, 152, doi: [10.3847/1538-4357/abb6fb](https://doi.org/10.3847/1538-4357/abb6fb)
- Ioka, K., & Zhang, B. 2020, *ApJL*, 893, L26, doi: [10.3847/2041-8213/ab83fb](https://doi.org/10.3847/2041-8213/ab83fb)
- Kirsten, F., Marcote, B., Nimmo, K., et al. 2022, *Nature*, 602, 585, doi: [10.1038/s41586-021-04354-w](https://doi.org/10.1038/s41586-021-04354-w)
- Klingler, N., Kargaltsev, O., Pavlov, G. G., et al. 2018, *ApJ*, 861, 5, doi: [10.3847/1538-4357/aac6e0](https://doi.org/10.3847/1538-4357/aac6e0)
- Lanman, A. E., Andrew, S., Lazda, M., et al. 2024, *AJ*, 168, 87, doi: [10.3847/1538-3881/ad5838](https://doi.org/10.3847/1538-3881/ad5838)
- Law, C. J., Bhardwaj, M., Burke-Spolaor, S., et al. 2024, *The Astronomer's Telegram*, 16701, 1
- Leahy, D. A., Darbro, W., Elsner, R. F., et al. 1983, *ApJ*, 266, 160, doi: [10.1086/160766](https://doi.org/10.1086/160766)
- Levin, Y., Beloborodov, A. M., & Bransgrove, A. 2020a, *ApJL*, 895, L30, doi: [10.3847/2041-8213/ab8c4c](https://doi.org/10.3847/2041-8213/ab8c4c)
- . 2020b, *ApJL*, 895, L30, doi: [10.3847/2041-8213/ab8c4c](https://doi.org/10.3847/2041-8213/ab8c4c)
- Lorimer, D. R., Bailes, M., McLaughlin, M. A., Narkevic, D. J., & Crawford, F. 2007, *Science*, 318, 777, doi: [10.1126/science.1147532](https://doi.org/10.1126/science.1147532)
- Lyutikov, M., Barkov, M. V., & Giannios, D. 2020, *ApJL*, 893, L39, doi: [10.3847/2041-8213/ab87a4](https://doi.org/10.3847/2041-8213/ab87a4)
- Maccarone, T. J., Kundu, A., Zepf, S. E., & Rhode, K. L. 2007, *Nature*, 445, 183, doi: [10.1038/nature05434](https://doi.org/10.1038/nature05434)
- Mannings, A. G., Fong, W.-f., Simha, S., et al. 2021, *ApJ*, 917, 75, doi: [10.3847/1538-4357/abff56](https://doi.org/10.3847/1538-4357/abff56)
- Ould-Boukattine, O. S., Hessels, J. W. T., Snelders, M. P., et al. 2024, *The Astronomer's Telegram*, 16732, 1
- Pearlman, A. B., Scholz, P., Bethapudi, S., et al. 2025, *Nature Astronomy*, 9, 111, doi: [10.1038/s41550-024-02386-6](https://doi.org/10.1038/s41550-024-02386-6)
- Postnov, K. A., & Yungelson, L. R. 2014, *Living Reviews in Relativity*, 17, 3, doi: [10.12942/lrr-2014-3](https://doi.org/10.12942/lrr-2014-3)
- Rajwade, K. M., Mickaliger, M. B., Stappers, B. W., et al. 2020, *MNRAS*, 495, 3551, doi: [10.1093/mnras/staa1237](https://doi.org/10.1093/mnras/staa1237)
- Ravi, V., Law, C. J., Li, D., et al. 2022, *MNRAS*, 513, 982, doi: [10.1093/mnras/stac465](https://doi.org/10.1093/mnras/stac465)
- Scargle, J. D. 1982, *ApJ*, 263, 835, doi: [10.1086/160554](https://doi.org/10.1086/160554)
- Shah, V., & CHIME/FRB Collaboration. 2024, *The Astronomer's Telegram*, 16670, 1
- Shah, V., Shin, K., Leung, C., et al. 2025, *ApJL*, 979, L21, doi: [10.3847/2041-8213/ad9ddc](https://doi.org/10.3847/2041-8213/ad9ddc)
- Sharma, K., Ravi, V., Connor, L., et al. 2024, *Nature*, 635, 61, doi: [10.1038/s41586-024-08074-9](https://doi.org/10.1038/s41586-024-08074-9)
- Sivakoff, G. R., Sarazin, C. L., & Jordán, A. 2005, *ApJL*, 624, L17, doi: [10.1086/430374](https://doi.org/10.1086/430374)
- Spitler, L. G., Cordes, J. M., Hessels, J. W. T., et al. 2014, *ApJ*, 790, 101, doi: [10.1088/0004-637X/790/2/101](https://doi.org/10.1088/0004-637X/790/2/101)
- Spitler, L. G., Scholz, P., Hessels, J. W. T., et al. 2016, *Nature*, 531, 202, doi: [10.1038/nature17168](https://doi.org/10.1038/nature17168)
- Sridhar, N., Metzger, B. D., Beniamini, P., et al. 2021, *ApJ*, 917, 13, doi: [10.3847/1538-4357/ac0140](https://doi.org/10.3847/1538-4357/ac0140)
- Stellingwerf, R. F. 1978, *ApJ*, 224, 953, doi: [10.1086/156444](https://doi.org/10.1086/156444)
- Szary, A., Melikidze, G. I., & Gil, J. 2015, *ApJ*, 800, 76, doi: [10.1088/0004-637X/800/1/76](https://doi.org/10.1088/0004-637X/800/1/76)
- Tendulkar, S. P., Gil de Paz, A., Kirichenko, A. Y., et al. 2021, *ApJL*, 908, L12, doi: [10.3847/2041-8213/abdb38](https://doi.org/10.3847/2041-8213/abdb38)
- Wada, T., Ioka, K., & Zhang, B. 2021, *ApJ*, 920, 54, doi: [10.3847/1538-4357/ac127a](https://doi.org/10.3847/1538-4357/ac127a)
- Wang, F. Y., Zhang, G. Q., Dai, Z. G., & Cheng, K. S. 2022, *Nature Communications*, 13, 4382, doi: [10.1038/s41467-022-31923-y](https://doi.org/10.1038/s41467-022-31923-y)
- Xu, K., Li, Q.-C., Yang, Y.-P., et al. 2021, *ApJ*, 917, 2, doi: [10.3847/1538-4357/ac05ba](https://doi.org/10.3847/1538-4357/ac05ba)
- Zanazzi, J. J., & Lai, D. 2020, *ApJL*, 892, L15, doi: [10.3847/2041-8213/ab7cdd](https://doi.org/10.3847/2041-8213/ab7cdd)
- Zhang, B. 2020, *Nature*, 587, 45, doi: [10.1038/s41586-020-2828-1](https://doi.org/10.1038/s41586-020-2828-1)

APPENDIX

A. EXPOSURE ANALYSIS AND PERIOD VALIDATION

The periodic analysis of FRB signals detected by CHIME requires careful consideration of potential aliasing effects due to the telescope’s constrained daily observing window of approximately 74 minutes. The detected periodicity of $P_0 = 126.6$ days, corresponding to a frequency of $f_0 = 1/P_0 = 0.0079 \text{ day}^{-1}$, could potentially be aliased with frequencies given by $f_n = N f_{\text{sid}} \pm f_0$ (Kirsten et al. 2022), where N represents an integer and $f_{\text{sid}} = (0.99727 \text{ day})^{-1}$ denotes the sidereal frequency. For the first-order alias ($N = 1$), this yields potential frequencies of $f_1 \approx 0.995$ or 1.011 day^{-1} (corresponding to periods of approximately one day), while second-order aliasing ($N = 2$) would result in frequencies of $f_2 \approx 1.998$ or 2.014 day^{-1} (periods of approximately half a day). Our independent confirmation using different methods and clear signs of clustered burst activity makes the possible periodicity a valid case and not an artifact of aliasing.

Our analysis solely depends on the CHIME-FRB reported bursts. Law et al. (2024) monitored the source with the Very Large Array in two 2-hour segments on 2024-07-02 and 2024-07-05, even after the claimed active phase, and found no bursts at the observing frequency of 1-2 GHz. After 350 hours of monitoring, Ould-Boukattine et al. (2024) used the Westerbork RT-1 telescope to discover a single burst at 1.3 GHz at the peak activity of FRB 20240209A in October 2024. This may point to very frequency-specific activity for the FRB 20240209A. We encourage sensitive radio interferometers which are not bound in exposure times, to observe this source both in intensity and polarization in the next predicted activity period to independently confirm periodic activity in the FRB 20240209A.

The FRB shows rapid clustering in the second and third activity epoch, which can lead to faulty estimation of the periodicity and create instabilities in the periodicity detection methods. To properly account for it, we have binned the time of arrivals assuming different averaging factors of 1, and 8 days and ran Lomb-Scargle analysis for all of them. We have allotted the mean time of arrival for each of the sampled bins. From the fig. 3 and table 1, all of the binned methods produce consistent results and hint towards a periodic activity of ~ 120 days.

Method	Periodicity
Autocorrelation Functions	$128.5 \pm 6 \text{ days}$
Epoch Folding	$128.8 \pm 14 \text{ days}$
Lomb-Scargle Periodogram (Unbinned)	$119.0 \pm 13 \text{ days}$
Lomb-Scargle Periodogram (1 Day Binned)	$119.3 \pm 14 \text{ days}$
Lomb-Scargle Periodogram (8 Days Binned)	$117.5 \pm 14 \text{ days}$

Table 1. Summary table showing all the explored periodicity finding methods and their results

B. BURST PROPERTIES

The burst properties such as their detection dates, detection DM and SNR are mentioned in the following table as taken from the CHIME repeaters’ database.

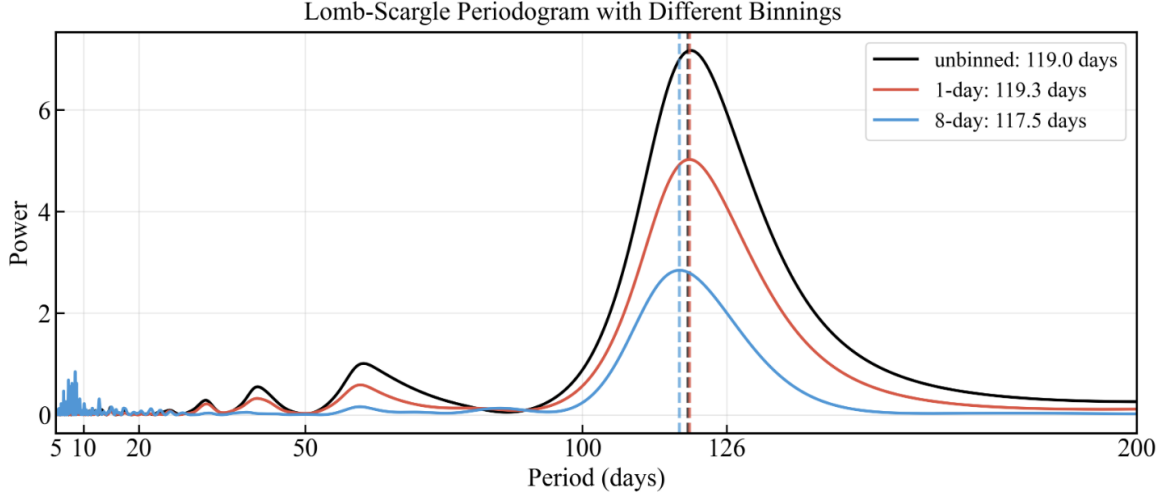


Figure 3. Comparison of Lomb-Scargle Periodogram analysis between unbinned (black), 1 day and (red) 8 days (blue) binning.

Burst ID	Event time	DM (pc cm ⁻³)	SNR
1	2024-02-09 07:10:14.629273	179.542 ^{+1.617} _{-1.617}	15.986
2	2024-02-17 06:36:05.165683	178.329 ^{+0.404} _{-0.404}	9.240
3	2024-03-01 02:39:49.031907	179.542 ^{+1.617} _{-1.617}	9.549
4	2024-03-09 04:29:37.491817	175.903 ^{+0.404} _{-0.404}	16.778
5	2024-06-08 10:23:09.135605	175.903 ^{+0.404} _{-0.404}	9.003
6	2024-06-08 10:23:09.143470	179.542 ^{+1.617} _{-1.617}	9.067
7	2024-06-12 08:51:06.703933	178.733 ^{+0.809} _{-0.809}	14.422
8	2024-06-12 21:33:20.540160	179.542 ^{+1.617} _{-1.617}	10.885
9	2024-06-15 07:55:53.038292	179.542 ^{+1.617} _{-1.617}	11.173
10	2024-06-16 22:52:19.363123	175.094 ^{+0.404} _{-0.404}	13.696
11	2024-06-19 08:57:36.594419	175.903 ^{+0.404} _{-0.404}	10.456
12	2024-06-19 09:03:37.417282	175.498 ^{+0.809} _{-0.809}	10.730
13	2024-06-19 10:11:00.873141	177.116 ^{+0.809} _{-0.809}	10.305
14	2024-06-20 08:55:51.754186	177.116 ^{+0.809} _{-0.809}	8.467
15	2024-06-20 09:14:46.669934	177.116 ^{+0.809} _{-0.809}	8.530
16	2024-06-21 21:00:56.070438	178.733 ^{+0.809} _{-0.809}	9.019
17	2024-06-25 20:20:30.661627	175.498 ^{+0.809} _{-0.809}	12.294
18	2024-06-28 22:05:21.265331	177.116 ^{+0.809} _{-0.809}	9.587
19	2024-06-29 07:58:35.964083	177.116 ^{+0.809} _{-0.809}	16.166
20	2024-06-29 08:32:47.395548	175.094 ^{+0.404} _{-0.404}	20.667
21	2024-06-29 08:57:55.017149	175.094 ^{+0.404} _{-0.404}	19.458
22	2024-06-29 11:07:02.025088	172.263 ^{+0.809} _{-0.809}	9.700
23	2024-06-29 19:16:34.348024	177.116 ^{+0.809} _{-0.809}	16.118
24	2024-07-02 08:36:06.603689	178.733 ^{+0.809} _{-0.809}	9.250
25	2024-07-16 06:14:15.889723	173.881 ^{+0.809} _{-0.809}	8.604
26	2024-10-13 00:51:21.915730	175.094 ^{+0.404} _{-0.404}	10.814
27	2024-10-13 15:05:04.347392	176.307 ^{+1.617} _{-1.617}	13.233
28	2024-10-15 01:54:43.840624	175.094 ^{+0.404} _{-0.404}	16.650
29	2024-10-16 13:03:56.155627	177.116 ^{+0.809} _{-0.809}	11.842
30	2024-10-17 13:48:36.063242	175.498 ^{+0.809} _{-0.809}	10.588

Table 2. FRB 20240209A Bursts' Properties

Burst ID	Event time	DM (pc cm ⁻³)	SNR
31	2024-10-19 01:33:14.245499	175.903 ^{+0.404} _{-0.404}	9.287
32	2024-10-20 01:41:40.400015	179.542 ^{+1.617} _{-1.617}	13.980
33	2024-10-21 00:44:11.257702	174.285 ^{+0.404} _{-0.404}	8.588
34	2024-10-22 00:40:36.301260	177.116 ^{+0.809} _{-0.809}	14.014
35	2024-10-22 12:23:55.770519	175.498 ^{+0.809} _{-0.809}	13.396
36	2024-10-24 14:20:08.455547	175.903 ^{+0.404} _{-0.404}	15.214
37	2024-10-24 23:17:14.999736	175.498 ^{+0.809} _{-0.809}	14.078
38	2024-10-25 12:24:44.518492	174.285 ^{+0.404} _{-0.404}	12.371
39	2024-10-26 11:15:13.038387	177.116 ^{+0.809} _{-0.809}	17.424
40	2024-10-26 11:29:07.780905	175.094 ^{+0.404} _{-0.404}	9.295
41	2024-10-26 12:54:38.974453	175.498 ^{+0.809} _{-0.809}	16.704
42	2024-10-27 00:18:52.517918	175.498 ^{+0.809} _{-0.809}	9.461
43	2024-10-27 23:47:52.290683	175.498 ^{+0.809} _{-0.809}	8.947
44	2024-10-28 01:40:03.574507	174.285 ^{+0.404} _{-0.404}	10.873
45	2024-10-28 12:40:33.872658	175.498 ^{+0.809} _{-0.809}	15.379
46	2024-10-29 12:55:40.022220	175.903 ^{+0.404} _{-0.404}	15.839
47	2024-10-30 11:54:11.757394	175.498 ^{+0.809} _{-0.809}	15.802
48	2024-10-30 23:44:04.395468	176.307 ^{+1.617} _{-1.617}	16.868
49	2024-10-31 00:13:47.228948	174.285 ^{+0.404} _{-0.404}	9.444
50	2024-10-31 01:40:11.420149	175.094 ^{+0.404} _{-0.404}	11.622
51	2024-11-01 23:20:35.248916	177.116 ^{+0.809} _{-0.809}	8.638
52	2024-11-02 11:36:03.835873	175.498 ^{+0.809} _{-0.809}	9.359
53	2024-11-03 01:35:46.483988	174.285 ^{+0.404} _{-0.404}	10.116
54	2024-11-10 00:19:39.894546	179.542 ^{+1.617} _{-1.617}	10.872
55	2024-11-19 10:53:51.946974	175.498 ^{+0.809} _{-0.809}	10.537
56	2024-11-24 00:08:12.294917	175.498 ^{+0.809} _{-0.809}	10.689
57	2024-11-26 22:50:30.653373	179.542 ^{+1.617} _{-1.617}	12.537
58	2025-01-09 19:47:17.250759	176.307 ^{+1.617} _{-1.617}	12.339
59	2025-01-26 19:12:53.510651	173.072 ^{+1.617} _{-1.617}	10.779
60	2025-01-28 18:52:21.264112	182.777 ^{+1.617} _{-1.617}	9.378
61	2025-02-05 17:37:48.015301	175.498 ^{+0.809} _{-0.809}	8.766
62	2025-02-11 07:11:26.067768	174.285 ^{+0.404} _{-0.404}	8.793
63	2025-02-19 18:41:39.946511	173.477 ^{+0.404} _{-0.404}	14.402
64	2025-02-28 16:34:35.754672	175.498 ^{+0.809} _{-0.809}	12.300

Table 3. FRB 20240209A Bursts' Properties